

THERMODYNAMIC ANALYSIS OF WATER BOILING IN PRESENCE OF A NON-CONDENSABLE GAS, THE CARBON DIOXIDE (CO₂): APPLICATION TO GEOTHERMAL FLOWS IN WELLBORES.

Thiagalingam I.*, Bergez W. and Colin C.
IMFT, INPT, UPS, CNRS, Université de Toulouse,
2 Allée Camille Soula,
F-31400 Toulouse,
France,
E-mail: ilango.thiagalingam@imft.fr

ABSTRACT

WID is a wellbore simulator developed as part of the GEOTREF (GEOThermal energy in Fractured REservoirs) project. A coupled system of equations ensuring mass, momentum and heat balance with appropriate set of models and correlations is resolved to describe multi-component and multi-phase flow along the well axis. The simulator is designed to be effective as a practical tool in the monitoring of geothermal systems. In the present work, the code is used to carry out physical investigations on the water boiling occurring alongside the degassing of a non-condensable gas, the carbon dioxide (CO₂). For high Reynolds flows in geothermal wellbores, it is illustrated that a thermodynamical approach with appropriate assumptions is able to accurately capture the effect of local physical mechanisms (such as the interfacial mass transfer resistance) on the global dynamic (partitioning of CO₂ in liquid and gas phases).

INTRODUCTION

The energy challenge is one of the greatest issues we are to face in the near future. The need to satisfy the increasing demand in energy and to significantly reduce at the same time our environmental impact in order to fight against the global warming issue, leads us to develop sustainable energy for large scale supply. Geothermal energy can be seen as a part of the solution as it has very low impact on the environment (almost no greenhouse gas emission) and high rate of availability. However, the field finds it difficult to attract stockbroking for mainly two reasons:

- Great risk to the investor at the upstream part of the project: very high drilling cost, geological risks remain high (exploration & prospecting cost) and very little investment from public organizations (strategy & funding)
- The very low price of fossil energy (oil, gas, coal)

The present work is part of the GEOTREF project, a multidisciplinary platform for innovation and demonstration activities for the exploration and development of high GEOThermal energy in Fractured REservoirs, financially supported by the French gov-

ernment. It has for ambition the development of innovative and practical tools to trigger private investments into the field [8]. The project consists in improving our understanding of fractured geothermal reservoirs during exploration and production phases. It can be divided into two parts. On the one hand, developing innovative tools that would help industrials to carry out reliable feasibility and exploitation studies and smartly manage a reservoir at the production state. On the other hand, providing a demonstration in Guadeloupe (French West Indies in the Antilles islands of the Caribbean) so as to prove the practical capabilities of developed tools. Thus, a positive reinforcement is spread, expecting that it would stimulate investments in the geothermal field.

The interest on multi-component systems raised among the geothermal professional community as soon as the pure water approximation was not able to give a satisfactory description of recorded pressure and temperature profiles in wells. Indeed, dissolved non-condensable gas, even in low amounts, has a significant impact on the boiling onset conditions. It increases for instance the vapor pressure of water leading to early flashing in geothermal production wells. Several codes have then been developed to simulate multi-component systems. One can mention for instance the EWASG module for the TOUGH2 reservoir simulator [3; 4] or the wellbore simulator PROFILI [5] based on the work of [2]. Reactive chemical transport has also been considered by [6; 7]. The effect of the non-condensable gas is included in wellbore codes [2] and enables to capture the correct flashing point along the well.

In this paper, we will focus on the physical aspect of the boiling in presence of a non-condensable gas. The wellbore flow model is first derived and validated on recorded data from Japanese wells[9]. Then the model to describe the effect of a non-condensable gas on the boiling mechanisms is presented and validated on recorded data from the well NG11 (Ngawa field, New Zealand) [10]. Finally, physical investigations are carried out to portray the complex thermodynamical path followed by the boiling of a pure fluid when it is coupled to the degassing of

NOMENCLATURE

Z	[m]	position along the well from the bottom
G	[kg/s]	mass flow rate
P	[Pa]	Pressure
T	[°C]	Temperature
Eu	[-]	Euler number
g	[m/s ²]	gravitational acceleration
Fr	[-]	Froud number
Ec	[-]	Eckert number
f	[-]	friction factor
H	[J/Kg]	mass enthalpy
Q	[W/m]	heat loss
Nu	[-]	Nusselt number
D	[m]	well diameter
Re	[-]	Reynolds number
U	[m/s]	velocity
h_w	[W/°C/m]	effective thermal conductivity
l	[m]	length of the well
x	[-]	steam quality
L	[J/kg]	latent heat
S	[-]	slip ratio
X	[-]	mass fraction
K_H	[Pa]	constant of Henry
m	[kg]	mass
M	[kg/mol]	molar mass

Special characters

ρ	[kg/m ³]	density
θ	[degree]	deviation angle from the vertical direction
ϵ	[m]	roughness
μ	[kg/m/s]	dynamic viscosity
α	[-]	void fraction
ψ	[-]	two-phase frictional multiplier
λ	[-]	vaporisation number

Subscripts

p	[-]	phase: 1 or v
$1p$	[-]	single phase
0	[-]	inlet
F	[-]	formation
w	[-]	wall
l	[-]	liquid
v	[-]	vapor
av	[-]	averaged over the well length
m	[-]	phase average
f	[-]	at flashing onset
g	[-]	gas
tot	[-]	total in both liquid and gas phases
i	[-]	interface
b	[-]	bulk

Superscripts

sat	[-]	saturation
$2p$	[-]	two-phase
$H2O$	[-]	water
$CO2$	[-]	carbon dioxide

a non-condensable gas.

W1D, A WELLBORE SIMULATOR FOR GEOTHERMAL APPLICATIONS

In this section, the model describing the flow in the well is presented, considering that the fluid is pure water. The main assumptions are similar to those used for the wellbore simulator FloWell [17]. For the single phase flow conditions, surface averaged (over the pipe cross section) mass, momentum and energy balance equations can be written as follows,

$$\frac{d}{dZ} \tilde{G} = 0 \quad (1)$$

$$\frac{d}{dZ} \frac{1}{\tilde{\rho}_p(P,T)} = -\frac{d\tilde{P}}{dZ} Eu - \frac{\tilde{\rho}_p(P,T) \cos(\theta) \tilde{g}}{Fr} - \frac{f_{1p}}{2\tilde{\rho}_p(P,T)} \quad (2)$$

$$\frac{d}{dZ} \left[\tilde{H} + \frac{Ec}{2\tilde{\rho}_p^2(P,T)} \right] + \frac{Ec}{Fr} \cos(\theta) \tilde{g} = -\frac{\tilde{Q}}{Nu} \quad (3)$$

using the following dimensionless quantities,

$$\begin{aligned} \tilde{G} &= \frac{G}{G_0}; & \tilde{Z} &= \frac{Z}{D}; & \tilde{\rho}_p(P,T) &= \frac{\rho_p(P,T)}{\rho_{p,0}(P_0,T_0)} \\ \tilde{P} &= \frac{P-P_0}{P_0}; & \tilde{g} &= \frac{g}{g_0} = 1; & \tilde{Q} &= \frac{Q}{Q_{av}}; & \tilde{H} &= \frac{H_p}{H_{p,0}} \end{aligned}$$

and dimensionless numbers,

$$\text{Euler number, } Eu = \frac{P_0 \pi^2 D^4 \rho_{p,0}}{16 G_0^2};$$

$$\text{Froud number, } Fr = \frac{16 G_0^2}{\pi^2 D^5 \rho_{p,0}^2 g};$$

$$\text{Eckert number, } Ec = \frac{16 G_0^2}{\pi^2 D^4 \rho_{p,0}^2 H_{p,0}};$$

$$\text{Reynolds number, } Re = \frac{4 G_0}{\pi \mu_{p,0} D};$$

Nusselt number, $Nu = \frac{4 G_0 H_{p,0}}{Q_{av} D}$ (which is the ratio between the convective heat flux at the well bottom and the mean heat flux in the formation considering that the fluid temperature within the wellbore is at the bottom hole temperature).

f_{1p} is the friction coefficient and it is given by the Swamee-Jain relation[11],

$$f_{1p} = \frac{0.25}{\left(\log\left(\frac{\epsilon}{3.7D} + \frac{5.74}{Re(Z)^{0.9}} \right) \right)^2} \quad (4)$$

The heat flux Q is estimated using a conduction model,

$$Q(Z) = 4h_w [T(Z) - T_F(Z)] \quad (5)$$

with $T_F(Z)$, the averaged temperature of the rock surrounding the well at the depth Z and h_w the effective thermal conductivity which being not known in principle, is usually treated as a parameter (its value is usually estimated to lie between 2 and 5 W/°C/m which is the underground rock average thermal conductivity). Q_{av} is an averaged heat loss along the tube length ($\frac{1}{l} \int_l 4h_w [T_0 - T_F(Z)] dZ$).

As for the two-phase flow conditions, surface averaged mass, momentum and energy balance equations can be written as follows,

$$\frac{d}{d\tilde{Z}} \tilde{G} = 0 \quad (6)$$

$$\frac{d}{d\tilde{Z}} \left[\frac{x^2}{\tilde{\rho}_v \alpha} + \frac{1-x^2}{\tilde{\rho}_l (1-\alpha)} \right] + Eu \frac{d\tilde{P}}{d\tilde{Z}} + \frac{\tilde{\rho}_m \tilde{g}}{Fr} + \frac{f_{1p}}{2\tilde{\rho}_l} \Psi^{2*} = 0 \quad (7)$$

$$\begin{aligned} \frac{d}{d\tilde{Z}} \left[\tilde{L}_{lv} \lambda x + \tilde{H}_l^{sat} + Ec^{2p} \left(\frac{x^3}{2\alpha^2 \tilde{\rho}_g^2} + \frac{(1-x)^3}{2(1-\alpha)^2 \tilde{\rho}_l^2} \right) \right] \\ + \frac{Ec^{2p}}{Fr} \cos(\theta) \tilde{g} = -\frac{\tilde{Q}}{Nu^{2p}} \end{aligned} \quad (8)$$

where $\tilde{\rho}_m$, H_l^{sat} and L_{lv} are respectively the phase averaged density, the enthalpy of the liquid at saturation conditions and the latent heat of vaporisation, $\tilde{\rho}_j = \rho_j / \rho_{l,0}$ with j standing for l (liquid), v (vapor) and m (phase averaged density), $\Psi^{2*} = \frac{\Psi^2}{6}$ with the two-phase frictional multiplier Ψ^2 is given by Friedel in [12]. Thermodynamic equilibrium enables to express the steam quality x as follows,

$$x(Z) = \frac{H(Z) - H_l^{sat}(Z)}{L_{lv}(T^{sat})} \quad (9)$$

Ec^{2p} is the two-phase Eckert number

$$Ec^{2p} = \frac{16G_0^2}{\pi^2 D^4 \rho_{l,0}^2 H_{l,f}^{sat}} \quad (10)$$

Nu^{2p} is the two-phase Nusselt number (it is the ratio between the convective heat flux at the flashing onset and the mean heat flux in the formation considering that the fluid temperature within the wellbore is at the bottom hole temperature)

$$Nu^{2p} = \frac{4G_0 H_{l,f}^{sat}}{Q_{av} D} \quad (11)$$

and λ is the vaporisation number,

$$\lambda = \frac{L_{lv,f}}{H_{l,f}^{sat}} \quad (12)$$

where $L_{lv,f}$ and $H_{l,f}^{sat}$ are evaluated using thermodynamic conditions at the flashing onset. The vaporisation number can be

viewed as the ratio between the energy needed to boil a unit mass of liquid and the available energy at the flashing onset.

To close the above system of equations, one needs to come up with a correlation for the void fraction α . The common method consists in relating the void fraction to the steam quality and to the slip ratio $S = U_v / U_l$. This can be achieved rewriting the phase averaged velocity,

$$\alpha = \frac{1}{1 + \left(\frac{1-x}{x}\right) \frac{\rho_v}{\rho_l} S} \quad (13)$$

and using a model for S [13].

$$S = 0.4 + 0.6 \sqrt{\frac{\rho_l}{\rho_v}} \left[\frac{1 + 0.4(\rho_v / \rho_l)(1-x)/x}{1 + 0.4(1-x)/x} \right]^{0.5} \quad (14)$$

The simulator W1D is validated comparing calculated pressure profiles to recorded ones in the Japanese wells [9]. A validation case is presented in Figure 1 for the well KE1-22. At the bottom of the well, the entering fluid is liquid. It boils within the well and exits at the head in annular regime.

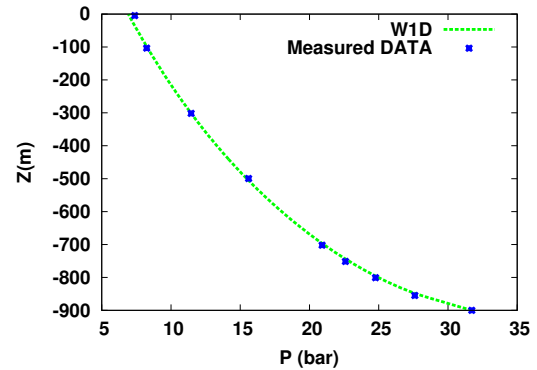


Figure 1. Well KE1-22: Dashed line is the computed pressure profile whereas symbols are the measured data.

WATER BOILING INDUCED BY THE DEGASSING OF CO_2

In this section a thermodynamical approach is undertaken to describe the water boiling in presence of a dissolved non-condensable gas (CO_2).

Model description

We assume that the amount of dissolved gas is small. Thus, the effect of CO_2 on the liquid phase density and viscosity is neglected. We also assume that the enthalpy of CO_2 and the heat of solution (the enthalpy change when dissolving the gas in a solvent) are negligible compared to the enthalpy of the liquid and vapor phases of water as well as in front of the latent heat.

Assuming that the gas phase is a mixture of independent ideal

gases, density and viscosity of the gas phase read

$$\rho_g(T^{sat}) = \rho_g^{H2O}(P^{H2O}, T^{sat}) + \rho_g^{CO2}(P^{CO2}, T^{sat}) \quad (15)$$

$$\mu_g(T^{sat}) = (1 - X_g^{CO2})\mu_g^{H2O}(P^{H2O}, T^{sat}) + X_g^{CO2}\mu_g^{CO2}(P^{CO2}, T^{sat}) \quad (16)$$

where P^{H2O} and P^{CO2} are the partial pressures of water and carbon dioxide respectively. X_g^{CO2} is the mass fraction of carbon dioxide in the gas phase. The density of carbon dioxide is computed using the correlation of Pritchett et al.[1]. As for the viscosity of the carbon dioxide, a fit of the data tabulated by [14] is obtained with the analytical form presented in [15].

The saturation condition is defined by

$$P = P^{H2O,sat}(T) + P^{CO2}(T, X_l^{CO2}) \quad (17)$$

Within the well and above the boiling onset location, the degassing of CO_2 in conjunction with the water boiling occurs and one can deduce at any location, the partial pressure of CO_2 using Eq.17,

$$P^{CO2}(T, X_l^{CO2}, Z) = P(Z) - P^{H2O,sat}(T, Z) \quad (18)$$

One can deduce the mass fraction of carbon dioxide in the liquid phase using the law of Henry (K_H is the constant of Henry),

$$X_l^{CO2}(Z) = \frac{(P^{CO2}/K_H)M^{CO2}}{(P^{CO2}/K_H)M^{CO2} + (1 - (P^{CO2}/K_H))M^{H2O}} \quad (19)$$

and the mass fraction of CO_2 in the gaseous phase using the law of Dalton.

$$X_g^{CO2}(Z) = \frac{P^{CO2}}{P(Z)} \quad (20)$$

The steam quality is defined as

$$x^{H2O} = \frac{m_g^{H2O}}{m_g^{H2O} + m_l^{H2O}} = \frac{1}{1 + \frac{m_l^{H2O}}{m_g^{H2O}}} \quad (21)$$

From the definition of the mass fraction of water in the liquid phase,

$$X_l^{CO2} = \frac{m_l^{CO2}}{m_l^{H2O} + m_l^{CO2}} \quad (22)$$

one gets,

$$\frac{m_l^{H2O}}{m_l^{CO2}} = \frac{X_l^{H2O}}{1 - X_l^{H2O}} = \frac{X_l^{H2O}}{X_l^{CO2}} \quad (23)$$

With the same reasoning,

$$\frac{m_g^{H2O}}{m_g^{CO2}} = \frac{X_g^{H2O}}{X_g^{CO2}} \quad (24)$$

Then, combining Eqs. 23 and 24,

$$\frac{m_l^{H2O}}{m_g^{H2O}} = \frac{m_l^{CO2}}{m_g^{CO2}} \frac{X_l^{H2O}}{X_l^{CO2}} \frac{X_g^{CO2}}{X_g^{H2O}} \quad (25)$$

Using the definition of the quality of CO_2 , one can substitute m_l^{CO2}/m_g^{CO2} by $(1 - x^{CO2})/x^{CO2}$. Finally,

$$\frac{m_l^{H2O}}{m_g^{H2O}} = \frac{1 - x^{CO2}}{x^{CO2}} \frac{1 - X_l^{CO2}}{X_l^{CO2}} \frac{X_g^{CO2}}{1 - X_g^{CO2}} \quad (26)$$

Substituting Eq.26 in Eq.21, and after rearrangement, one obtains the following expression for the steam quality,

$$x^{H2O}(Z) = \frac{x^{CO2} X_l^{CO2} (1 - X_g^{CO2})}{x^{CO2} X_l^{CO2} (1 - X_g^{CO2}) + X_g^{CO2} (1 - X_l^{CO2}) (1 - x^{CO2})} \quad (27)$$

It states that when the degassing of CO_2 starts ($x^{CO2} > 0$), it induces boiling ($x^{H2O} > 0$).

The quality of CO_2 can be assessed using once again the law of Henry,

$$\frac{P^{CO2}}{K_H} = \frac{G^{CO2} (1 - x^{CO2}) / M^{CO2}}{G^{CO2} (1 - x^{CO2}) / M^{CO2} + G^{H2O} (1 - x^{H2O}) / M^{H2O}} \quad (28)$$

with G^{CO2} and G^{H2O} the mass flow rates of total CO_2 and total water respectively. They are related to the mass flow rate of the mixture G following $G^{CO2} = X_{tot}^{CO2} G$ and $G^{H2O} = (1 - X_{tot}^{CO2}) G$ where X_{tot}^{CO2} is the total mass fraction of CO_2 (in the liquid and gas phases). Eq. 28 becomes then

$$\frac{P^{CO2}}{K_H} = \frac{X_{tot}^{CO2} (1 - x^{CO2}) / M^{CO2}}{X_{tot}^{CO2} (1 - x^{CO2}) / M^{CO2} + (1 - X_{tot}^{CO2}) (1 - x^{H2O}) / M^{H2O}} \quad (29)$$

Replacing the steam quality by Eq.27 and after rearrangement,

one obtains a quadratic equation for the CO_2 quality,

$$\begin{aligned} (x^{CO_2})^2 + x^{CO_2} \left[\frac{X_l^{CO_2}(1 + X_g^{CO_2}) - 2X_g^{CO_2}}{X_g^{CO_2} - X_l^{CO_2}} + \frac{(P^{CO_2}/K_H)(M^{CO_2}/M^{H_2O})(1 - X_0^{CO_2})X_g^{CO_2}(1 - X_l^{CO_2})}{(X_g^{CO_2} - X_l^{CO_2})X_{tot}^{CO_2}(1 - P^{CO_2}/K_H)} \right] \\ + \left(1 - \frac{(P^{CO_2}/K_H)(M^{CO_2}/M^{H_2O})(1 - X_{tot}^{CO_2})}{X_{tot}^{CO_2}(1 - (P^{CO_2}/K_H))} \right) \times \\ \frac{X_g^{CO_2}(1 - X_l^{CO_2})}{X_g^{CO_2} - X_l^{CO_2}} = 0 \end{aligned} \quad (30)$$

The physical solution of the above equation reads,

$$\begin{aligned} x^{CO_2}(Z) = -0.5 \left[\frac{X_l^{CO_2}(1 + X_g^{CO_2}) - 2X_g^{CO_2}}{X_g^{CO_2} - X_l^{CO_2}} + \frac{(P^{CO_2}/K_H)(M^{CO_2}/M^{H_2O})(1 - X_{tot}^{CO_2})X_g^{CO_2}(1 - X_l^{CO_2})}{(X_g^{CO_2} - X_l^{CO_2})X_{tot}^{CO_2}(1 - P^{CO_2}/K_H)} \right] \\ - 0.5 \left\{ \left[\frac{X_l^{CO_2}(1 + X_g^{CO_2}) - 2X_g^{CO_2}}{X_g^{CO_2} - X_l^{CO_2}} + \frac{(P^{CO_2}/K_H)(M^{CO_2}/M^{H_2O})(1 - X_{tot}^{CO_2})X_g^{CO_2}(1 - X_l^{CO_2})}{(X_g^{CO_2} - X_l^{CO_2})X_{tot}^{CO_2}(1 - P^{CO_2}/K_H)} \right]^2 \right. \\ \left. - 4 \frac{X_g^{CO_2}(1 - X_l^{CO_2})}{X_g^{CO_2} - X_l^{CO_2}} \left(1 - \frac{(P^{CO_2}/K_H)(M^{CO_2}/M^{H_2O})(1 - X_{tot}^{CO_2})}{X_{tot}^{CO_2}(1 - (P^{CO_2}/K_H))} \right) \right\}^{0.5} \end{aligned} \quad (31)$$

The total quality is defined as

$$x = \frac{m_g^{H_2O} + m_g^{CO_2}}{m_g^{H_2O} + m_l^{H_2O} + m_g^{CO_2} + m_l^{CO_2}} \quad (32)$$

$$= \frac{m_g^{CO_2}(1 + m_g^{H_2O}/m_g^{CO_2})}{\left(\frac{m_g^{H_2O} + m_l^{H_2O}}{m_g^{CO_2} + m_l^{CO_2}} + 1 \right) (m_g^{CO_2} + m_l^{CO_2})} \quad (33)$$

$$= \frac{x^{CO_2}/X_g^{CO_2}}{1 + \frac{m_g^{H_2O}}{x^{H_2O}(m_g^{CO_2} + m_l^{CO_2})}} \quad (34)$$

with

$$\frac{m_g^{H_2O}}{m_g^{CO_2} + m_l^{CO_2}} = x^{CO_2} \frac{m_g^{H_2O}}{m_g^{CO_2}} = x^{CO_2} \frac{X_g^{H_2O}}{1 - X_g^{H_2O}} \quad (35)$$

After rearrangement, one is able to end up with

$$x(Z) = \frac{x^{CO_2} x^{H_2O}}{x^{CO_2} + X_g^{CO_2}(x^{H_2O} - x^{CO_2})} \quad (36)$$

$$H_l^{H_2O,sat}(Z) = -[H_g^{H_2O,sat}(Z) - H_l^{H_2O,sat}(Z)]x^{H_2O}(Z) + H_{l,f} \quad (37)$$

where $H_{l,f}^{H_2O}$ and H_l^{sat} are the enthalpies respectively at the boiling onset location Z_f and at the the location Z .

From the steam quality the saturation water enthalpy can be deduced, that gives the temperature T^{sat} along the well in two-phase regime (the converged T^{sat} is obtained iteratively: the loop starts with Eq.18 and ends with the estimated T^{sat} by Eq.37. Until the relative difference between the mass fraction of CO_2 (Eq.20) estimated with the initial temperature and the one estimated by Eq.37 is lower than 1%, the loop is maintained with the initial temperature refreshed with the estimated one.

Validation and Discussion

The model is validated comparing simulations to measured pressure and temperature profiles in the well NG11 (Ngawa field, New Zealand) [10]. One can first notice in Figs. 2 and 3 that tacking into account the presence of the dissolved gas with the recommended value for the non-condensable mass fraction (1.2% of CO_2 [10]) gives better agreement with the measured data than the pure water assumption.

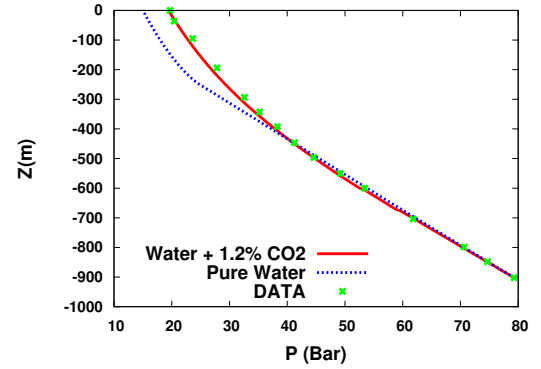


Figure 2. Computed pressure profile vs. measured data in well NG11.

The other point which is interesting to notice is the early onset of the boiling with the presence of a non-condensable gas (the temperature is virtually constant in the single liquid phase and then decreases after the boiling incipience). Indeed, the typical effect of the non-condensable gas is to increase the saturation pressure for a given temperature. The actual model seems to predict the shift of the boiling onset quite accurately. It is worthwhile to notice that unlike the pure water boiling for which the knowledge of the pressure is sufficient to deduce the temperature, a boiling in conjunction with a degassing requires besides the amount of CO_2 remaining dissolved in the liquid phase to have access to the temperature. This information was obtained above from a thermodynamical consideration. The complex thermodynamical path is drawn in a PT diagram which differs from the usual saturation curve for the pure water boiling (see Fig 4). The saturation curve of a water containing 1.2% of dissolved CO_2 is

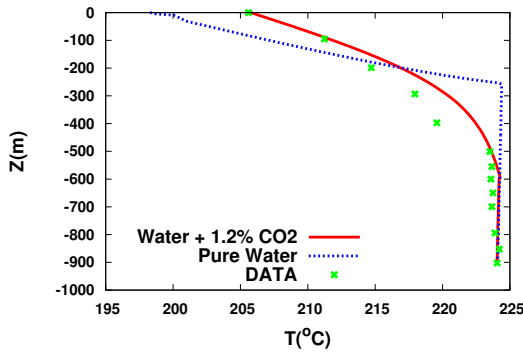


Figure 3. Computed temperature profile vs. measured data in well NG11.

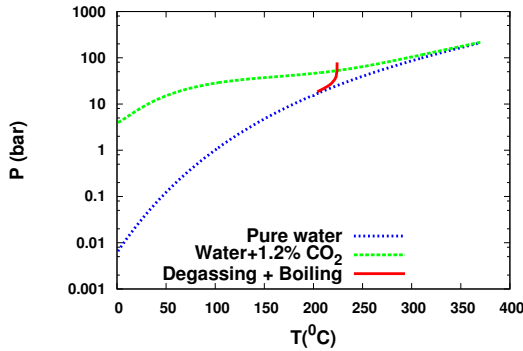


Figure 4. Saturation curves for the pure water and the water containing 1.2% of CO_2 are represented with dashed lines. The solid line pictures the thermodynamical path followed by the fluid during its upward flow in well NG11.

drawn with green dashed line. It lies above the saturation curve of the pure water, implying the onset of boiling at higher pressure for a given temperature. The well is fed by liquid water and its flow along the well without heat transfer with the surrounding rock is represented by a downward vertical line. As soon as it crosses the green dashed line, degassing is started triggering the boiling (see Eq. 21 which states that a non-zero quality of CO_2 leads to a non-zero vapor quality). When the degassing in conjunction with the boiling is progressing along the well, it follows the path drawn in Fig. 4 that is obtained invoking thermodynamical equilibrium of ideal mixture of gases.

Although the non-condensable mass fraction in the liquid phase is very small, its relative weight in the gas phase can be very important (Figs.5 and 6). For instance, it represents around 70% of the gas phase weight just above the boiling onset location in the well. It strongly supports that the degassing process prevails over the steam evaporation in the early stage of the vaporisation process (see also in Fig.4 the quasi-vertical slope dP/dT along the thermodynamical path). The weight of the non-condensable gas gradually diminishes in the gas phase but remains important all along the well: indeed, even at the outlet

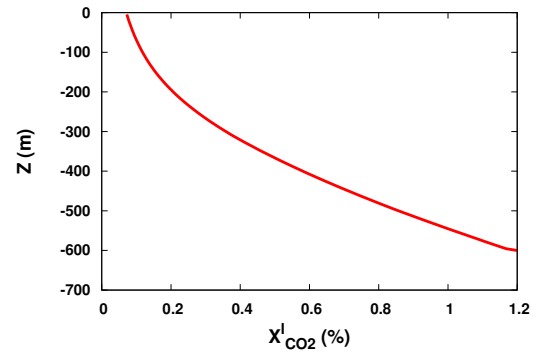


Figure 5. Evolution of the mass fraction of CO_2 in the liquid phase.

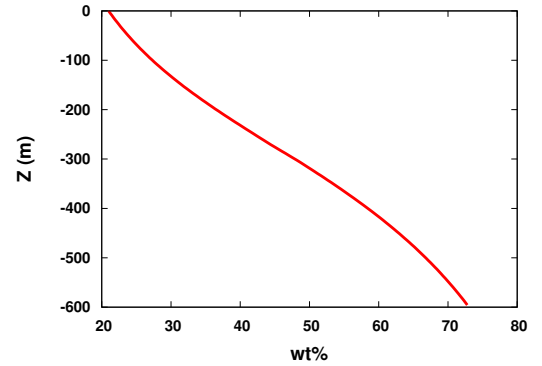


Figure 6. Evolution of the mass fraction of CO_2 in the gas phase.

of the well, the mass fraction of the non-condensable gas represents around 22% in the gas phase.

The kinetic of the degassing process is driven only by the pressure drop as it is assumed to be isothermal. As evidenced in Fig.7, its kinetic is much more efficient than the kinetic of boiling. Effectively, the quality of CO_2 is reaching almost 95% at the head of the well whereas the vapor quality remains low (around 5%). A closer look at the local gas-liquid interface is necessary to understand it. Indeed, the more volatile gas is CO_2 and its concentration is higher at the interface than in the bulk liquid creating hence a mass transfer resistance that reduces the steam evaporation rate at the interface [16]. It results in a smooth vaporization when it occurs in conjunction with the CO_2 degassing compared to the case where the pure water is boiling alone . In Fig. 8, whereas in the pure water boiling case the fluid undergoes an abrupt phase change passing from the liquid phase to a froth flow regime in less than fifty meters, in the case where there is a small amount of CO_2 dissolved in the water, the evolution of the void fraction is made smoother by the mass transfer resistance that maintains a reduced vaporisation by elevating the interface temperature above the bulk liquid temperature. In other words, the excess energy released by the pressure drop is not sufficient to water molecules (which would have left the liquid phase if there

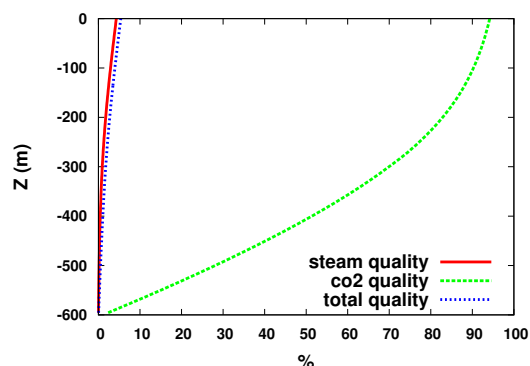


Figure 7. Evolution of steam, CO_2 and total qualities.

were no CO_2) to free from the surrounding ones and quit the liquid phase when CO_2 molecules are located at the liquid-gas interface in higher proportion than in the bulk liquid ($T - T_i < T - T_b$). Then only a reduced amount of water molecules quits the liquid phase compared to the case where there is no CO_2 molecules at the interface. This local effect seems well captured by the constant of Henry. Effectively, the turbulent diffusion is assumed high enough to lead quasi-instantaneous migration of CO_2 molecules from bulk to the interface so as to reach the thermodynamical equilibrium predicted by the law of Henry.

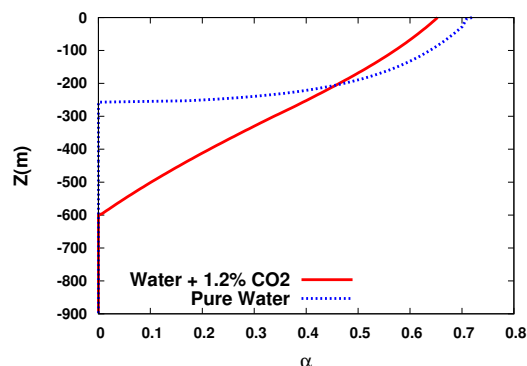


Figure 8. Evolution of the void fraction along the well.

CONCLUSION

As part of the GEOTREF project, a wellbore simulator W1D is developed. The mathematical model is based on the mass, momentum and energy balance. The partitioning of water and CO_2 molecules between gas and liquid phases is assessed seeking instantaneous thermodynamical balance between species in each phases. From the present work it can be noticed that when boiling occurs in conjunction with the degassing of a non-condensable gas, the thermodynamical path followed by the multi-component and multi-phase system is more complex. However, seeking for a global thermodynamical equilibrium, one is able to capture quite accurately the dynamic of the process as it was shown here with the case studied above (flow in a geothermal well).

Besides, the present work is shedding light on the thermodynamical coupling between two distinct processes enabling to assess quantitatively the partitioning of each species between liquid and gas phases all along the well. The validity of the constant of Henry for different two-phase flow regimes encountered in geothermal wells is the key point which enabled the thermodynamical equilibrium approach to be successful in the description of the process.

The above investigations suggest that an addition of a small amount of non-condensable gas could be considered to smooth water boiling process which would prevent from explosive vaporization.

References

- [1] J. W. Pritchett, M. H. Rice and T. D. Riney, Equation-of-state for water-carbon dioxide mixtures: implications for Baca reservoir. *Report DOE/ET/27163-8*, UC-66a, La Jolla, CA, 1981.
- [2] A. Barelli, R. Corsi, G. Del Pizzo and C. Scali, A two-phase flow model for geothermal wells in the presence of non-condensable gas, *Geothermics*, Vol. 11, No. 3, 1982, pp. 175-191.
- [3] A. Battistelli, C. Calore and K. Pruess, A fluid property module for the TOUGH2 simulator for saline brines with non-condensable gas, *Proceedings 18th Workshop on Geothermal Reservoir Engineering*, Stanford, CA, 1993, pp. 249-259.
- [4] A. Battistelli, C. Calore and K. Pruess, The simulator TOUGH2/EWASG for modeling geothermal reservoirs with brines and non-condensable gas, *Geothermics*, Vol. 26, No. 4, 1997, pp. 437-464.
- [5] A. Battistelli, PROFILI code: the thermodynamic package for $H_2O-NaCl-CO_2$ fluid mixtures, *Aquater Report H 6046*, San Lorenzo in Campo, Pesaro, Italy, 1991.
- [6] S. P. White, Transport of reacting chemicals in a two-phase reservoir, *Proceedings 16th New Zealand Geothermal Workshop*, Auckland, 1994, pp. 175-180.
- [7] S. P. White, Multiphase non-isothermal transport of systems of reacting chemicals, *Water Resources Research*, Vol. 32, 1995, pp. 1761-1772.
- [8] www.geotref.com
- [9] S. K. Garg, J. W. Pritchett and J. H. Alexander, Development of new geothermal wellbore holdup correlations using flowing well data, Idaho National Engineering and Environmental Laboratory, report of march 2004.
- [10] A. Battistelli, J. Rivera, R. and C. Ferragina, The modeling of flow in geothermal wells applied to the reservoir engineering study of the Asal Field Republic of Djibouti, *13th annual PNOC-EDC Geothermal Conference*, Feb. 19-21, 1992.
- [11] P. K. Swamee and A. K. Jain, Explicit equations for pipe-flow problems, *J. Hydraulics Division*, Vol. 102, No. 5, 1979, pp. 657-664.
- [12] J. Friedel, Improved friction pressure drop correlations for horizontal and vertical two-phase pipe flow, *European two-phase flow group meeting*, Ispro, Italy, 1979.
- [13] D. Chisholm, *Two-phase flow in pipelines and heat exchangers*, George Godwin, London and New York, 1983.
- [14] N. B. Vargaftik, *Handbook of Physical Properties of Liquids and Gases*, Springer-Verlag Berlin Heidelberg, 1975.
- [15] S. P. Aunzo, G. Bjornsson and G. S. Bodvarsson, Wellbore Models GWELL, GWNACL, and HOLA, User's Guide, Lawrence Berke-

- ley Laboratory, University of California, 1991.
- [16] S. G. Kandlikar, Boiling heat transfer with binary mixtures: Part I - a theoretical model for pool boiling, *ASME*, Vol. 120, 1992.
- [17] H. Gudmundsdottir and M. T. Jonsson, The wellbore simulator FloWell - Model enhancement and verification, Proceedings World Geothermal Congress, Melbourne, Australia, 2015.